Monitoring of Rotor Bar Faults in Induction Generators with Full-Size Inverter

Goran Stojičić[1], Matthias Samonig[1], Peter Nussbaumer[1], Gojko Joksimović[2], Mario Vašak[3], Nedjeljko Perić[3], Thomas M. Wolbank[1]

[1] Department of Electrical Drives and Machines, Vienna University of Technology, Austria

[2] Faculty of Electrical Engineering, University of Montenegro Podgorica, Montenegro

[3] Faculty of Electrical Engineering and Computing, University of Zagreb, Croatia

thomas.wolbank@tuwien.ac.at

Acknowledgment - The work to this paper was supported by the European Union in the SEE-ERA.NET PLUS framework.

«condition monitoring, fault diagnosis, induction machines, rotor broken bar faults, transient excitation»

Abstract - Monitoring of generators is an essential part when operating a plant in remote areas. Nowadays demands on system reliability are very high and thus maintenance at regular intervals is necessary. Standard fault detection methods are usually based on several additional sensors. Such monitoring systems increase system costs and afford an additional source of fault. To avoid this disadvantage an alternative technique based only on the usage of sensors already available in the power inverter will be shown. The method is based on machine's response due to voltage pulses generated by inverter switching. Measurement of the current response and subsequent signal processing leads to very detailed information about the machine state. Identification and separation of machine asymmetries obtained from two subsequent Fast Fourier Transformations offer a high sensitive fault indicator. The generation of the excitation pulses, current sampling and the signal processing chain as well will be described. Measurements for several levels of rotor bar fault severity are presented and the fault detection sensitivity and efficiency is proven.

I. Introduction

To keep overall energy efficiency high, control of generator speed and torque is realized using power electronics. Demands on system reliability are very high and thus currently maintenance at regular intervals is necessary. Operation of generators under extreme conditions with respect for example to temperature, vibration, and moisture like in a wind turbine combined with fast switching power electronics devices lead to considerably reduced reliability of the overall system. Costs of maintenance and risk of unexpected failure can significantly be reduced by online condition monitoring. In the past, several methods were presented in the area of online fault detection. The majority of the methods focus on sidebands of stator current as fault indicator. Therefore different spectrum analysis methods such as wavelet approaches like [1], [2] and [3], Fourier transforms [4], Hilbert transforms [5] or neuronal networks [6], [7] where published. These methods are based on machine's current signature-analysis (MCSA). Alternative methods are introduced in [8], [9] where the fault indicator is based on active and reactive power spectra analysis or line to line voltage spectra [10] or time frequency distributions [11]. All these methods are usually limited to steady-state or slow changing machine operations. However, the operation of generators in different applications is predominantly transient, therefore prompting the development of fault detection methods capable of handling non-stationary or transient operation modes. The main focus is to increase reliability and reduce costs by applying methods and fault indicators that can allow continuous monitoring of critical components without the need for expensive additional sensors and measurement equipment. The method should get along with sensors already available in the inverter as well as with different control loops. In addition, the most important result in online condition monitoring is not just to obtain fault information when a specific component already broke down thus significantly reducing operability. In order to allow maintenance on-demand it is important to generate a warning message already when a deterioration of the component is detected indicating that a breakdown will happen in the near future. Reducing stress on early stage detected faults leads to a slow down of fault development and the life

cycle can be extended. For example, a method for fault-tolerant control in wind turbine generators at developing rotor bar faults is given in [11].

The fault mechanism analyzed in the following investigation is a developing breakage of a rotor bar in an induction generator. The online monitoring is based on the excitation of the machine with voltage pulses generated by the switching of the inverter and measuring the current response. When applying voltage pulses to the terminals of a machine, using the different output states of a voltage source inverter the resulting current change will be dominated by the transient leakage inductance, which can be identified and used as a fault indicator after further signal processing steps. As mentioned, the focus of this investigation is laid on rotor faults in inverter fed induction machines, but the principles of the method can as well be used for detecting stator winding shortcircuits and eccentricities between stator and rotor in induction machines as well as permanent magnet synchronous machines.

II. Transient Leakage Inductance and Machine's Asymmetries

A. Estimation of the Transient Leakage Inductance

In the following, the configuration of the signal processing will be described. The method is based on the detection of the current reaction caused by a voltage step applied to the machine terminals. The voltage step is produced by changing the voltage source inverter switching state. The length of the voltage step is some 10µs. The current measurement is realized by the built-in current sensors at two different time instants during each pulse.

The reaction of an ideal symmetrical machine can be described with the stator equation (1).

$$\underline{v}_S = r_S \cdot \underline{i}_S + l_l \cdot \frac{d\underline{i}_S}{d\tau} + \frac{d\underline{\lambda}_R}{d\tau} \tag{1}$$

The dominant voltage drops of the short voltage step are the time derivate of the rotor flux $\underline{\lambda}_R$ (machines back emf) and the leakage inductance l_l times the time derivate of the stator current $\underline{i}_S$. As the stator current and its time derivative (difference) is directly measured, the dominating disturbance according to (1) is the machine back emf that has to be eliminated. This elimination is realized by applying two different subsequent voltage pulses. The voltage pulses are denoted with index *I* and *II*. As already described, the time duration of the voltage pulse is very short therefore the magnitude and direction of the back emf will not change noticeable. The elimination of the back emf is then performed by subtraction of the two step responses. The fundamental wave point of operation will remain almost unchanged if a special (symmetrical) switching pattern is applied. Therefore the influence of the stator resistance voltage drop can be eliminated by this subtraction too. The resulting equation is presented in (2) where the index *t* of the leakage inductance indicates its transient value.

$$\underline{v}_{S,I} - \underline{v}_{S,II} = l_{l,t}\left(\frac{d\underline{i}_{S,I}}{d\tau} - \frac{d\underline{i}_{S,II}}{d\tau}\right) \tag{2}$$

If a fault is developing in a machine, the transient leakage is no longer a scalar but gets a complex value. It's components are a symmetrical l_{offset} and a complex portion $\underline{l}_{\text{mod}}$ representing the fault induced asymmetry with its magnitude and spatial direction. The angle of the complex portion also gives the spatial position of the asymmetry corresponding to the direction of maximum inductance.

$$\underline{l}_{l,t} = l_{offset} + \underline{l}_{\text{mod}}, \quad \underline{l}_{\text{mod}} = l_{\text{mod}} \cdot e^{j2\gamma} \tag{3}$$

If (3) is inserted in (2) and the resulting equation is inverted, then the number of necessary mathematical operations for the evaluation process is reduced what leads to (4).

$$\frac{\Delta\underline{i}_{S,I-II}}{\Delta\tau} = y_{offset} \cdot \left(\underline{v}_{S,I-II}\right) + \underline{y}_{mod} \cdot \left(\underline{v}^{*}_{S,I-II}\right) \tag{4}$$

The overall inverse transient leakage inductance can now easily be calculated from the known voltage phasor $\underline{v}_{S,I-II}$ and the measured current derivate. As already shown, this inverse value contains a symmetrical portion (denoted *offset*) and asymmetrical one (denoted *mod*). The symmetrical one corresponds to the mean inductance value and the corresponding share of the current difference leads

to a measured overall current difference in the direction of the difference voltage phasor. The asymmetrical one corresponds with the asymmetry introduced by the fault, which in this investigation equals a broken bar. Thus the offset value has to be eliminated for sensitive fault detection. This can be realized by subsequent excitation in different phase directions. After adding up the resulting current differences the symmetrical component caused by the offset is eliminated and the remaining phasor represents the machine asymmetries. A more detailed description of the procedure is given in [13].

B. Machines Asymmetries

The value of the symmetrical portion I_{offset} only depends on the fundamental-wave point of operation. The whole excitation and measurement process is completed in some 10 µs. The change of the fundamental-wave in this time period is negligible. Thus the value of I_{offset} can be identified by the combination of excitations in three different phase directions. The simplest way to do this is to apply the voltage pulses to the three main phase directions of the machine. Adding up the three current response phasors leads to a zero component of the current phasor. The remaining phasor ($\underline{\nu}_{s,I\text{-}II}\cdot\underline{\nu}_{mod}$) is now only asymmetry dependent and in the following denoted as asymmetry phasor. This phasor contains information about the machine's asymmetries. In addition to the fault induced asymmetry there are also further inherent asymmetries superposed in the asymmetry phasor. These asymmetries are present in every machine if faultless or not and are caused by saturation, slotting and anisotropy of the rotor.

The main part of inherent asymmetries is dominated by the saturation saliency. It is caused by a modulation of the level of saturation along the circumference of the machine. The modulation period is twice that of the fundamental wave what corresponds to the number of poles in the machine. The magnitude of the saturation saliency is flux and load dependent and the angular position is linked with the fundamental wave.

Corresponding to the machine design there is a rotor slotting dependent modulation. The reason is caused by the openings of the rotor slots and the period is equal the number of rotor slots. The influence from the operating point of the machine on this asymmetry part is negligible and the magnitude is only geometry dependent.

III. Signal Processing and Fault Indicator

A. Fault Induced Asymmetry

To establish fault detection a fault indicator has to be developed. Therefore inherent saliency components must be removed from the asymmetry phasor. This separation is challenging and the base for fault detection. Therefore some specific signal processing steps have to be done which are presented in the following. But before setting up the measurement and signal processing the behavior of the fault induced saliency must be examined.

Stator-slot leakage and zigzag flux, passing the air gap to bridge the slot openings of both stator and rotor, are the main components of the transient flux linkage. In a symmetrical machine the rotor cage has a relative long electrical time constant of typically some hundred milliseconds. It prevents any transient changes of the rotor flux by blocking the transient flux to the rotor surface. In case of a broken bar the zigzag flux can avoid the slot openings by passing the rotor slot below the broken bar. The position of this asymmetry in the transient flux linkage is corresponding to the mechanical angle of the rotor. Assuming a four pole machine the broken bar induced asymmetry leads to a modulation with a period equal to the number of poles. The modulation caused by the saturation saliency also has a period corresponding to the number of poles. Thus the fault induced asymmetry will be detectable with the same spatial period as the saturation harmonic. For fault detection these two asymmetries have to be separated. The necessary signal processing steps are explained in the following chapter.

B. Signal Processing for Asymmetry Separation

Now as the behavior of the fault asymmetry is known, separation of saturation saliency and fault modulation is performed by specific signal processing steps. For a better understanding of the signal processing Fig 1 depicts a block diagram of the method.

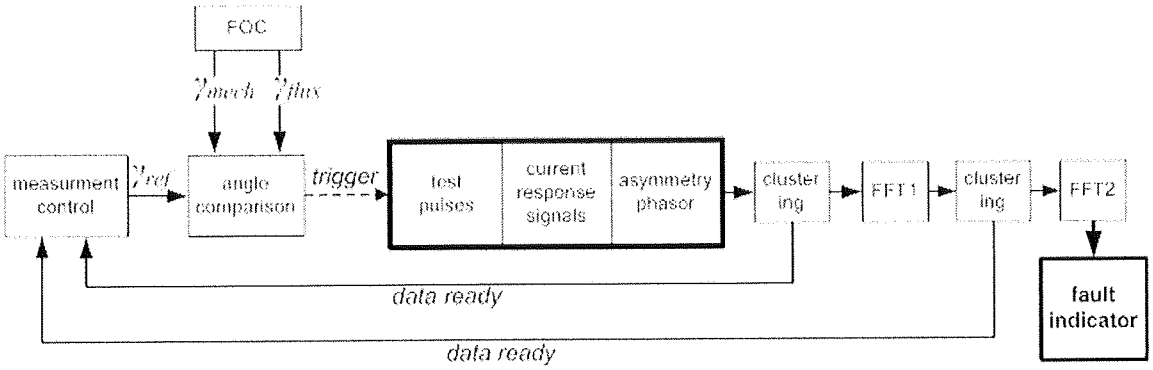

Fig 1: Block diagram of proposed method (signal processing steps)

The measurement control decides when a fault examination has to be done. In a first step a set of reference angle values is generated. Each set γ_{ref} consists of two values one for the mechanical and one for the electrical angle. These values are forwarded where they are compared (angle comparison) with the actual rotor γ_{mech} and flux angle γ_{flux} obtained from the field oriented control (FOC). When the rotor and flux position match with γ_{ref} a trigger signal is set. This leads to an excitation of the machine with voltage pulses and the measurement of the resulting current differences as described above (current response signals). Finally, a phasor is calculated according to (4). In Fig 1 these steps are indicated by a thick black rectangle. The estimated phasor now is the asymmetry phasor which is the base for further signal processing. Subsequently the phasor is shifted to the first clustering block and stored. After that a "data ready" signal is send to the measurement control and a new set of γ_{ref} values is generated. Thereby only the mechanical angle reference is increased while the flux angle remains unchanged. This procedure is repeated until a set of asymmetry phasor values is obtained with respect to one mechanical revolution.

In the next step the stored asymmetry phasor set is forwarded to the first Fast Fourier Transform FFT1 and a spectrum is calculated. As described above, all phasor values are estimated at the same flux angel with respect to the stator surface but different rotor positions. Thus the window length of FFT1 is one mechanical revolution. Fig 2 depicts the harmonic content of the asymmetry phasor set as a result of FFT1. The investigated machine has two pole-pairs and a rotor with 28 bars. Operating point of the machine was rated flux and 50% load at 70% rated speed with a faulty rotor cage. As can be clearly seen in the diagram the rotor slotting causes a high -28^{th} harmonic together with a $+28^{th}$ harmonic. Due to the measurement and signal processing procedure (same flux position for all asymmetry phasor values) the saturation saliency has no modulation and is represented in the offset, denoted saturation. The influence of the faulty bar is repeated for every pole. Hence, the fault induced harmonic is equal the $+4^{th}$.

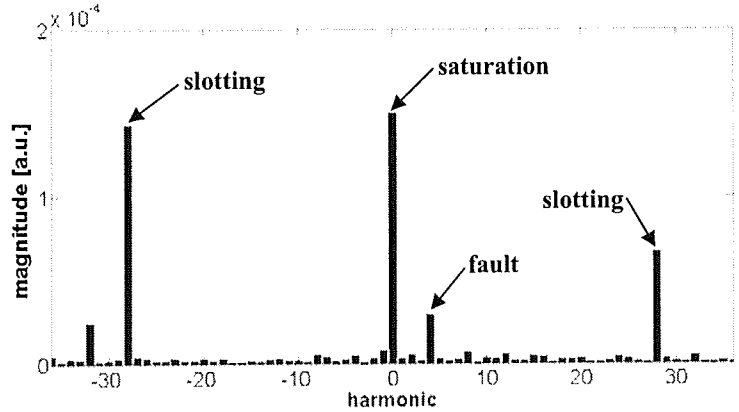

Fig 2: Spectrum of the asymmetry phasor as result of the first Fast Fourier Transform (FFT1).

Out of this spectrum only the fault induced harmonic value is sent to the second clustering block and a "data ready" signal is sent to the measurement control. Now the measurement control increases the reference value for the flux position and the estimation procedure for fault induced harmonic is executed again. These signal processing steps are repeated for several flux positions within one electrical revolution. Subsequently FFT2 can be calculated. As input values of FFT2 now only serve

the different fault induced harmonics for different flux positions and the window length is one electrical revolution. The offset value of FFT2 serves now as indicator for the rotor bar fault level. Therewith other parasitic modulations are eliminated.

IV. Measurement Setup and Results

As was shown in section II it is necessary to apply a specific transient excitation to the machine in order to obtain the asymmetry phasor information. Therefore short voltage pulses have to be generated and the current response be measured and further processed. The pulse generation is preferably done by inverter switching from one active output state to another. The trigger signals are generated by the control system. The system used is a real time computer system which drives the inverter and receives the current sample signals. The required voltage pulse excitation and current measurement procedure is depicted in Fig 3. The figure shows a symmetrical pulse excitation consisting of negative and positive inverter switching states in phase direction U (black line) and the current response signal (red line). As can be seen the fundamental wave operating point (represented by horizontal time axis) is almost unchanged due to the symmetrical nature of the pulse pattern. The subsequent voltage pulses for back emf elimination (2) are denoted as *pulse I* and *II* and the magnitude of the pulses is equal the dc-link value which can be considered constant during the excitation process. The estimation of the current derivative is done using the current difference $\Delta \underline{i}_S/\Delta\tau$ by taking two current samples during each pulse (gray dashed lines) and further calculation. Built-in current sensors of the inverter allow a simple current sampling.

As now the voltage phasor $\underline{v}_{S,I\text{-}II}$ and the current change signal are known (4) can be calculated easily. In a next step the offset value y_{offset} has to be eliminated. This is done by applying the excitation pulse sequence depicted to all three main phase directions subsequently and combining the current difference phasors to one resulting phasor. Hence one asymmetry phasor is obtained and the offset-component y_{offset} is eliminated.

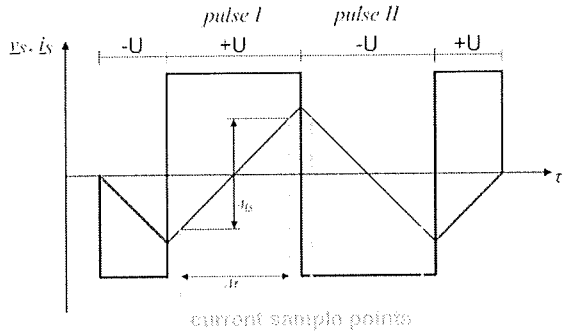

Fig 3: Pulse excitation in phase direction U and current sampling

Measurements were done on 5kW test machine with 4 poles, 36 stator slots and a squirrel cage rotor. The rotor was specially manufactured allowing to remove or change each of the 28 unskewed rotor bars. The bars are fixed on the end rings by inner and outer threads and screws. The common procedure to generate asymmetries in the rotor cage by drilling holes in lamination and bars can so be avoided. Rotor faults and beginning cracks are realized easily by changing one or more bars by bars made of other materials or by removing them. Thus even developing bar breakage can be simulated without destroying the rotor.

To establish a very high spatial resolution, the number of rotor positions for asymmetry phasor estimation and the first Fourier transform FFT1 is chosen to 256 values. For the second transform FFT2 the flux angle steps are distributed with 10° along the stator circumferences, so one window of saved 4th harmonics consists of 36 values.

The sensitivity of the investigated method is tested and verified by different measurements. First the machine is investigated in the symmetrical case. Therefore the rotor cage is symmetrical and all cage bars are made of solid copper. These measurements serve as reference. In order to examine the sensitivity of the method for different operation points of the machine, measurements are done for several load and speed levels.

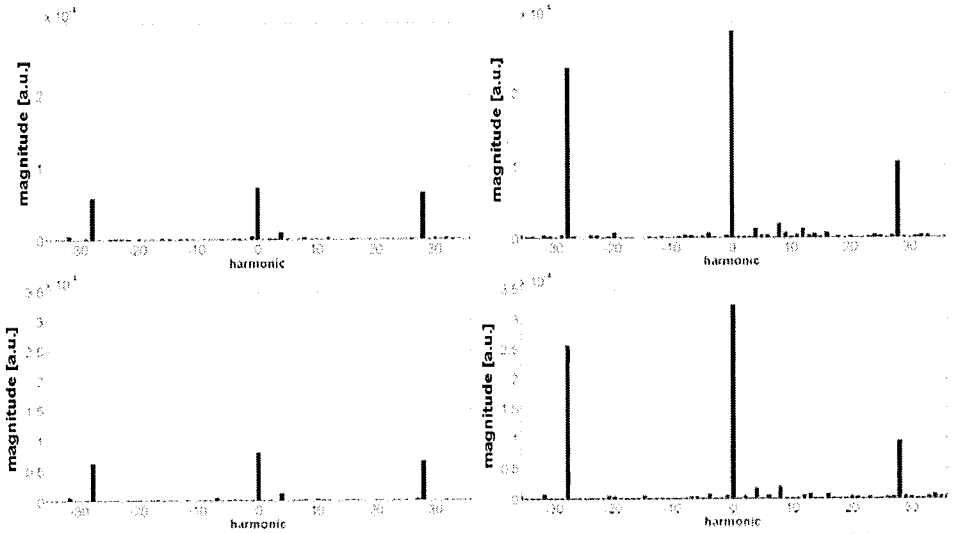

Fig 4: Spectrum of FFT1 for two load and two speed levels of a faultless machine.
Upper row: speed level 35%. Lower row: speed level 70%
Left: load level 25%(braking). Right: load level 70%(braking).

The speed levels are set 35% (525 rpm) and 70% (1050 rpm) rated speed. The special design of the rotor currently does not allow tests at higher speeds. Fig 4 depicts results of FFT1 for different speed and generator load levels. The upper row shows the spectra for 35% rated speed and the lower row for 70% rated speed. On the left side load was set to 25% and on the right side to 70% rated braking load torque. As can be seen, all relevant harmonics increase with higher load level but not noticeable with different speeds. A significant increase is clearly recognizable on the offset (saturation) as well as the -28^{th} harmonic (resulting from intermodulation of saturation and slotting). On the other side the $+28^{th}$ increases only marginally. Although in the actual case a faultless rotor is investigated a low $+4^{th}$ (fault induced) is still existing in all diagrams. This can be interpreted as a small asymmetry in the faultless rotor due to lamination anisotropy and a slight variation of the contact resistances between bars and end rings. This asymmetry remains constant till the rotor cage is reconfigured. In addition there are some further harmonics ($+8^{th}$, $+12^{th}$ ...) arising at higher load level. They have their reason in intermodulation of the fault modulation and saturation saliency. The magnitude values of the diagrams are given in arbitrary units [a.u.] corresponding to the internal representation of the control system.

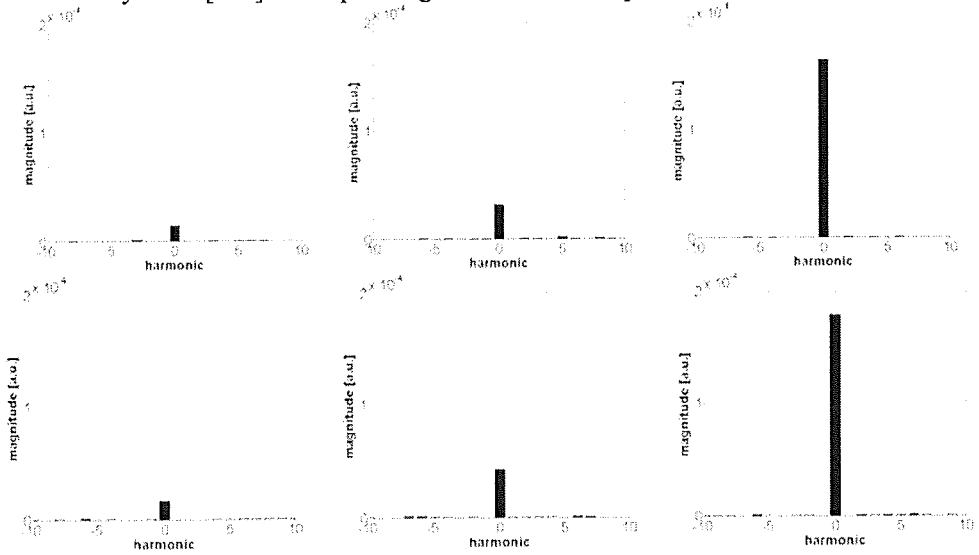

Fig 5: Fault indicator after FFT2 for different fault and speed levels. Load is set to 70%.
The machine is operated at 35% (upper row) and 70% (lower row) rated speed, respectively.
Left: faultless. Middle: brass bar. Right: broken bar.

To test the ability to detect a broken bar as well as a partially broken bar two different fault levels were investigated. In the case of a broken bar one bar was removed from the rotor cage. In the case of

a developing bar fault the resistance of one bar increases but a current path still exists. To reproduce such fault scenario a rotor bar with a higher resistance then a copper bar is applied. This fault level is generated by a bar made of brass. The resistance of a brass bar was measured to 374% higher than of a copper bar. Fig 5 shows the fault indicator for three different fault levels. On the left the faultless case in the middle the developing bar breakage (brass bar) and right the broken bar (removed bar) are shown. The upper row represents results at 35% rated speed and the lower at 70% rated speed.

The braking load in both cases is set to 70%. As already mentioned the offset of the second Fourier transform FFT2 serves as fault indicator. The figure depicts resulting diagrams of FFT2 for several measurements. A distinct growth of the offset magnitude is clearly detectable for increasing fault level (left faultless and right broken bar). The offset value in faultless case amount $0.14 \cdot 10^{-4}$ a.u. at lower speed and $0{,}16 \cdot 10^{-4}$ a.u. at higher speed. That of the brass bar $0.33 \cdot 10^{-4}$ a.u. and $0.43 \cdot 10^{-4}$ a.u., respectively. Finally for the broken bar $1.64 \cdot 10^{-4}$ a.u. and $1.79 \cdot 10^{-4}$ a.u.. As can be seen, the fault indicator increases in case of a change of the resistance in only one single bar about 2.3 times and in case of a broken bar even 11 times at 35% rated speed. On the other side the value is 2.5 times and 11 times higher at the higher speed. These results show that the fault indicator performance can be considered speed independent regarding the detection of a broken bar.

In Fig 4 the load dependence of the harmonic content is described. As was shown the impact of machine's speed on the fault indicator is negligible but magnitude of several harmonics as well as the fault indicator changes with different load levels. An investigation of these dependencies is done by some further measurements. Therefore the fault indicator is measured and calculated for a symmetrical cage, a cage with one bar made of brass and a removed bar at different load levels. The measurements are done at two different speed levels again.

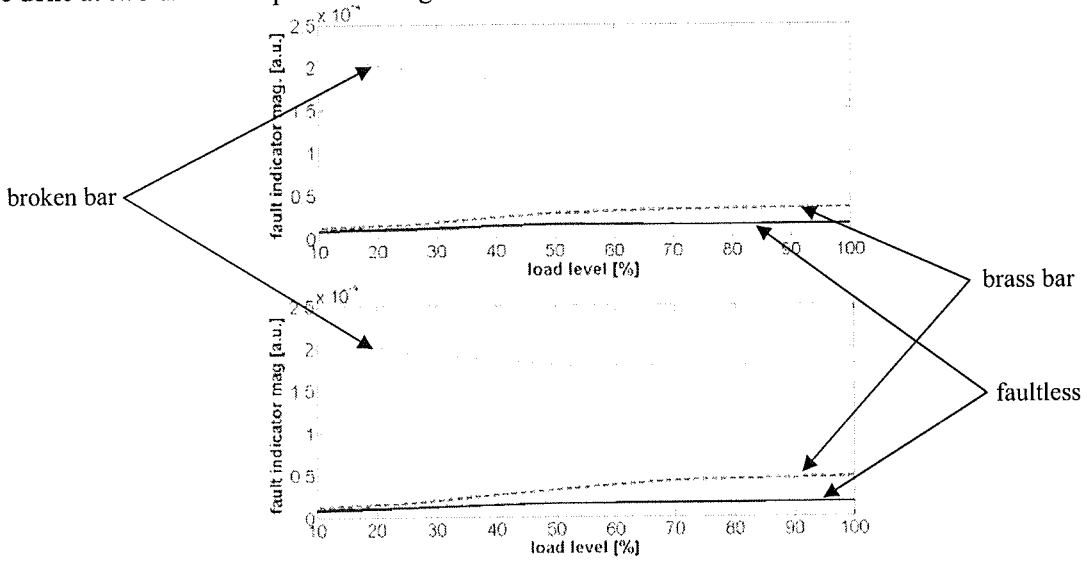

Fig 6: Fault indicator at different generator load levels.
(upper diagram machine speed: 35%; lower: machine speed:70%)

Fig 6 shows the measurement results. The fault indicator magnitude is plotted against the load level which is given in percent of rated load. In the upper diagram the machine was operated at 35% rated speed, in the lower at 70%. The results in the diagrams again approve the speed independence of the fault indicator. The values change only negligible between the two measurements. The blue line represents the fault indicator value for the faultless case. Its value is almost constant for the whole load range. The green, dashed line describes the developing bar damage (brass bar) and red the broken bar case. Both fault cases shows a slight load dependency of the fault indicator but nevertheless a fault can clearly be detected at every load level without the need for an additional load level compensation. This leads to the statement that detection of broken bars and even developing bar breakage is possible with the proposed measurement and signal processing setup in the whole load and speed range.

V. Conclusion

A method has been proposed to detect broken bar fault and even developing rotor bar fault in induction generators fed by full size inverters. The method affords satisfactory accuracy already in a

beginning state of a rotor bar fault. It is based on an excitation of the machine with voltage pulses caused by the switching of the inverter and the measurement of the resulting current reaction. The signal processing consists of two subsequent Fourier transforms and an intermediate clustering process to extract the fault indicator. Thus the fault induced asymmetry can be separated accurately from the inherent asymmetries and there is no need for a commissioning phase to identify especially the inherent saturation asymmetry. Measurements for different fault cases at several operating points have shown high sensitivity of the fault indicator at wide speed and load range of the generator. Using the method, a broken bar as well as even only an increase of a single rotor bar resistance of 374% can be clearly detected.

VI. References

[1] S.H. Kia, H. Henao and G. Capolino, "Diagnosis of Broken Bar Fault in Induction Machines Using Discrete Wavelet Transform without Slip Estimation," *IEEE Transactions on Industry Applications*, vol.45, no.4, pp.1395-1404, 2009.

[2] M. Riera-Guasp, J. A. Antonino-Daviu, M. Pineda-Sanchez, R. Puche-Panadero and J. Perez-Cruz, "A General Approach for the Transient Detection of Slip-Dependent Fault Components Based on the Discrete Wavelet Transform," *IEEE Transactions on Industrial Electronics*, vol.55, no.12, pp.4167-4180, 2008.

[3] W. Le Roux, R. G. Harley and T. G. Habetler, "Detecting Rotor Faults in Low Power Permanent Magnet Synchronous Machines," *IEEE Transactions on Power Electronics*, vol.22, no.1, pp.322-328, 2007.

[4] A. Bellini, A. Yazidi, F. Filippetti, C. Rossi and G. Capolino, "High Frequency Resolution Techniques for Rotor Fault Detection of Induction Machines," *IEEE Transactions on Industrial Electronics* vol.55, no.2, pp.4200-4209, 2008.

[5] M. Pineda-Sanchez, M. Riera-Guasp, J.A. Antonino-Daviu, J. Roger-Folch, J. Perez-Cruz and R. Puche-Panadero, "Instantaneous Frequency of the Left Sideband Harmonic During the Start-Up Transient: A New Method for Diagnosis of Broken Bars," *IEEE Transactions on Industrial Electronics,* vol.56, no.11, pp.4557-4570, Nov. 2009.

[6] B. Ayhan, M.-Y. Chow and M.-H. Song, "Multiple Discriminant Analysis and Neural-Network-Based Monolith and Partition Fault-Detection Schemes for Broken Rotor Bar in Induction Motors," *IEEE Transactions on Industrial Electronics*, vol.53, no.4, pp.1298-1308, 2006.

[7] F. Filippetti, G. Franceschini and C. Tassoni, "Neural networks aided on-line diagnostics of induction motor rotor faults," *IEEE Transactions on Industry Applications*, vol.31, no.4, pp.892-899, 1995.

[8] G.R. Bossio, C.H. De Angelo, J.M. Bossio, C.M. Pezzani and G.O. Garcia, "Separating Broken Rotor Bars and Load Oscillations on IM Fault Diagnosis Through the Instantaneous Active and Reactive Currents," *IEEE Transactions on Industrial Electronics,* vol.56, no.11, pp.4571-4580, Nov. 2009.

[9] M. Drif and A. J. Marques Cardoso, "Use of the instantaneous reactive-power signature analysis for rotor-cage-fault diagnostics in three phase induction motors," *IEEE Transactions on Industrial Electronics,* vol. 56, no. 11, pp. 4606–4614, Nov. 2009.

[10] A. Khezzar, M. El Kamel Oumaamar, M. Hadjami, M. Boucherma and H. Razik,"Induction Motor Diagnosis Using Line Neutral Voltage Signatures," *IEEE Transactions on Industrial Electronics,* vol.56, no.11, pp.4581-4591, Nov. 2009.

[11] S. Rajagopalan, J. Restrepo, J. Aller, T. Habetler, R. Harley, 'Nonstationary Motor Fault Detection Using Recent Quadratic Time–Frequency Representations', *IEEE Transactions on Industry Applications*, 735-744, May 2008.

[12] V. Lešić, M. Vašak, N. Perić, G. Joksimović and T. Wolbank, "Fault-Tolerant Control of a Blade-pitch Wind Turbine With Inverter-fed Generator",*Proceedings of IEEE International Symposium on Industrial Electronics,* ISIE, Jun. 2011.

[13] T. Wolbank, P. Nussbaumer, H. Chen and P. Macheiner, "Non-invasive detection of rotor cage faults in inverter fed induction machines at no load and low speed", *Proceedings of IEEE International Symposium on Diagnostics for Electric Machines, Power Electronics and Drives*, SDEMPED, pp.1-7, 2009.